Neuro-Oncology
19(4), 586–594, 2017 | doi:10.1093/neuonc/now193 | Advance Access date 15 September 2016

Radiation injury versus malignancy after stereotactic radiosurgery for brain metastases: impact of time-dependent changes in lesion morphology on MRI

Sabine Wagner, Heinrich Lanfermann, Gerrit Eichner, Hubert Gufler

Institute of Neuroradiology, Johann-Wolfgang-Goethe University Frankfurt, Frankfurt/Main, Germany (S.W., H.L.); Institute of Diagnostic and Interventional Neuroradiology, Hannover Medical School, Hannover, Germany (H.L.); Mathematical Institute, Justus-Liebig-University Giessen, Giessen, Germany (G.E.); Department of Diagnostic Radiology, Martin-Luther-University Halle-Wittenberg, Halle/Saale, Germany (H.G.); Department of Neuroradiology, Friedrich-Schiller-University Jena, Jena, Germany (S.W.)

Corresponding Author: Sabine Wagner, MD, Department of Neuroradiology, Friedrich-Schiller-University Jena, Erlanger Allee 101, 07747 Jena, Germany (sabine-m-wagner@gmx.de).

Abstract

Background. We sought to determine whether radiation-induced injuries could be distinguished from malignancy after stereotactic radiosurgery (SRS) by analyzing time-dependent changes in lesion morphology on sequential MRI for up to 55min.

Methods. In 31 consecutive patients treated with SRS for brain metastases, the time-dependent changes in lesion morphology were analyzed on MRI 2min, 15min, and 55min after contrast administration and on subtraction images. A simultaneous, matched-pairs approach was used for quantitative region of interest analysis of the area of the lesion. Qualitative analysis comprised the shape of the border, the structure of the interior area, the presence of leptomeningeal enhancement, and feeding vessels. The signal intensity changes of the border and the interior area of the lesions over time were assessed visually. The time-dependent changes in the 2 entities were compared.

Results. Twenty radiation-induced injuries and 21 malignancies were analyzed. A significant interaction effect between time point and diagnosis ($P<.001$) was found for the time-dependent changes of the margin of the lesion for 2min to 15min and in signal intensity differences of the rim and interior area as well as of the size of the interior area for up to 55min. All radiation-induced injuries showed a black interior area on the subtraction images for 15min minus 55min, whereas all malignant lesions had white components ($P<.001$).

Conclusions. Analysis of time-dependent changes in lesion morphology on sequential MRI for up to 55min is a reliable tool to distinguish radiation-induced injuries from malignancy after SRS.

Key words

brain metastases | delayed contrast MRI | lesion morphology | radiation injury | stereotactic radiosurgery

Tumor progression after stereotactic radiosurgery (SRS) to treat brain metastases requires that an optimal therapeutic strategy be chosen as early as possible.[1] In the follow-up of patients after SRS, distinguishing recurrent or progressive tumor from radiation-induced injuries on standard MRI is rather challenging. Although advanced MRI modalities such as perfusion imaging, MR spectroscopy, and PET may sometimes be helpful in distinguishing treatment effects from recurrent tumor,[2–8] most of these studies show a large overlap between the 2 disease entities. These approaches have not been able to replace histological verification of the diagnosis so far. This distinction, however, is clinically meaningful because radiation-induced injuries are often self-limited, and patients may benefit from symptomatic treatment alone, whereas if a tumor progresses, either SRS must be resumed or surgery, whole-brain radiation, or chemotherapy performed. To avoid stereotactic biopsy or open surgery, several investigators have attempted to define characteristic

Importance of the study

Sensitivity and specificity of morphologic MRI features were found to be low in retrospective radiographic-pathological studies to distinguish progressive tumor from radiation-induced injuries in the follow-up of patients after SRS for brain metastases. By applying our new concept, we analyzed the time-dependent changes in lesion morphology on contrast-enhanced MRI up to 55min after contrast administration. The time-dependent changes were statistically significantly different for the margin of a lesion, the size of the interior and total area, the signal intensity of the interior area, and the signal intensity contrast between the rim and the interior area. Subtraction images of 15min minus 55min provide information about the signal-intensity time-course differences at a glance: radiation-induced injuries show a homogeneous, dark interior area, whereas malignant lesions show white components. Assessment of the time-dependent changes in lesion morphology is helpful in planning therapy in the follow-up of patients after SRS.

lesion patterns on standard contrast-enhanced MRI to distinguish radiation injury from tumor progression. Unfortunately, either sensitivity or specificity for morphologic MRI features and patterns of enhancement was found to be low in retrospective radiographic-pathological studies.[9–11]

In the brain, MR signal changes caused by contrast agent extravasation are determined by several factors, including tissue perfusion, capillary permeability, and volume of extracellular spaces.[12] As the histopathological features of radiation-induced injuries and malignancies differ, the variables influencing contrast enhancement in the brain also differ. This might lead to different kinetics of the contrast medium over time with possible visualization on delayed images, so-called late gadolinium enhancement.[13]

By applying our concept, we analyzed the time-dependent changes in lesion morphology of contrast-enhancing lesions after SRS for brain metastases. The aim of our study was to determine whether radiation-induced injuries and malignancies are significantly different using quantitative and qualitative parameters which are relevant as known from the literature,[14–19] on sequential, contrast-enhanced MRI for up to 55min after contrast administration. As a second aim we evaluated the contribution of subtraction images for rapidly distinguishing between radiation-induced injuries and malignancy.

Materials and Methods

Study Design

Local institutional review board approval was received for this prospective single center study. Enrollment was restricted to patients previously treated with SRS for cerebral metastases with radiologically confirmed (i) presence of a contrast-enhancing lesion at the irradiated tumor site, (ii) a newly diagnosed brain metastasis on routine follow-up MR examinations, and (iii) final diagnosis established using conclusive radiological and clinical follow-up data. Final diagnoses were: radiation-induced injuries, tumor recurrences, and newly diagnosed metastases. Each participant gave written informed consent prior to inclusion. For SRS a Gamma Knife was used. The prescription dose was defined by coverage of the target volume, normally around 95% of the tumor volume. The dose was 20–25 Gy for small to medium brain metastases and lower for large metastases to avoid complications. Multiple isocenters were used to ensure that the dose distribution was highly conformal.

A continuously enlarging brain lesion located at or close to the SRS-treated tumor site with surrounding edema and mass effect was classified as tumor recurrence or tumor progression. An enhancing lesion was classified as radiation-induced injury if it was reversible and resolved with symptomatic treatment. Finally, a new, contrast-enhancing lesion in a region that had not been the target of SRS based on previous MRIs was diagnosed as distant recurrence.

MRI Data Acquisition

MR examination of the brain was performed in study participants on a 3-Tesla system (Magnetom Allegra, Siemens Medical Systems) with a quadrature 4-channel head coil. T1-weighted images were acquired at 3 different time points: 2min, 15min, and 55min after intravenous administration of a standard dose (0.1 mmol/kg) of gadolinium–diethylenetriamine pentaacetic acid. Signal intensity (SI) of cerebral metastases increases early after contrast agent administration,[20] and usually routine imaging is performed around 2min after contrast application. It has been reported that ischemic stroke and brain tumors have a second, slow delayed contrast extravasation at around 12min to 15min after contrast application.[21,22] Additionally, for analyzing late gadolinium enhanced MR studies it has to be assured that a diagnostically valid enhancement is still seen on the images.[23]

Data Processing and Image Evaluation

The original datasets were transferred for offline analysis. The image with the maximum cross-sectional diameter of an enhancing lesion was chosen and evaluated quantitatively and qualitatively for each of the three time points using the freely available software tool Xrayline Workstation 2.0. Subtraction images were generated for postcontrast 15min minus postcontrast 55min and postcontrast 55min minus postcontrast 15min conditions.

For quantitative analysis, polygonal regions of interest were drawn manually on the T1-weighted contrast-enhanced images to measure the entire areas of the contrast-enhancing lesion, the hyperattenuating rim, and

the hypoattenuating interior area. The regions of interest were placed precisely on corresponding positions for all images acquired at the three different time points.

Qualitative longitudinal analysis included: firstly, the shape of the border (sharp, blurred, and faded); secondly, the structure of the interior area (homogeneous, dotted, and septate); and, thirdly, the SI changes of the border and the interior area of the lesions (increase, no change, and decrease). Finally, the presence of leptomeningeal enhancement and feeding vessels was documented.

Qualitative assessments of the subtraction images 15min minus 55min and 55min minus 15min comprised the presence and the distribution of black and white components in the rim and the interior area of the lesion.

Statistics

For statistical analysis we used R Statistics software,[24] including the package lme4.[25] The time courses of the quantitative parameters were analyzed using a 2-level, linear, mixed-effects regression model.[26–28] The qualitative morphological parameters of the subtraction images of the 2 diagnostic groups were compared using Fisher's exact test. The quotient of the quantitative measurements was analyzed using the Wilcoxon-Mann-Whitney test, data from longitudinal observation of the qualitative parameters according to Brunner and Langer.[29] The family of *P*-values of those Fisher's tests and the Wilcoxon tests were adjusted for multiple testing using Holm's method.

Results

According to our inclusion criteria, 31 consecutive patients were prospectively enrolled in this study. The mean age of these patients was 50.4 years (range, 33–71 y). Sixteen of the 31 patients were men, 15 women. Primary tumor type/site was breast (8), lung (7), malignant melanoma (5), renal cell carcinoma (4), colorectal carcinoma (2), synovial sarcoma (1), and carcinoma of the testicles (1). The primary tumor location was unknown in 3 cases.

In all, 41 lesions met the defined diagnostic criteria using radiological and clinical follow-up data. The radiation-induced injury group consisted of 20 lesions; the malignancy group consisted of 9 tumor recurrences and 12 newly diagnosed metastases. In our study group, the mean interval between the end of SRS and the onset of radiation-induced injury was 9.3 months, ranging from 3 months to 22 months and for tumor recurrences 8.4 months (from 3 mo to 16 mo), respectively.

By applying our concept, the time-dependent changes are statistically significantly different for the disease entities for several parameters. Significant interaction effects between time point and diagnosis were revealed regarding the subtraction images: on subtraction images 15min minus 55min all radiation-induced injuries showed a homogeneous, black interior area of the lesion, whereas all malignant lesions had white components ($P < .001$) (Figs. 1, 2); this was accompanied by a predominance of the signal of the rim in the radiation-injury group (20/20) and of the interior area in the malignancy group (17/21) ($P < .001$). Analysis of the subtraction images 55min minus 15min was complementary: all radiation-induced injuries showed white components in the interior area of the lesion, whereas only 5 of 21 malignant lesions did ($P < .001$). The signal was predominant in the interior area in all lesions of the radiation-induced injury group and in the rim in 19 of 21 of the malignancy group ($P < .001$). The results are visualized in a fourfold display according to Friendly[30] in Fig. 3A. No significant difference was found on either subtraction image for the diagnostic groups regarding the

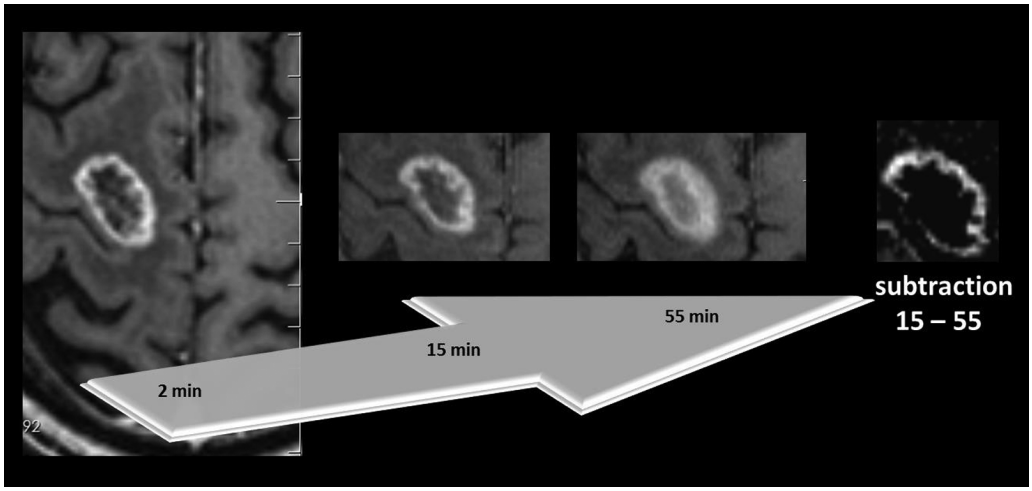

Fig. 1 Radiation-induced necrosis in a 49-year-old woman with SRS-treated brain metastasis from lung cancer. Axial T1-weighted MR images 2min, 15min, and 55min after contrast agent administration with subtraction image 15min minus 55min.A homogeneous black inner area of the lesion is seen in the subtraction image without any white components. Progressive "fill in" up to 55min is seen with increasing SI in the inner area.

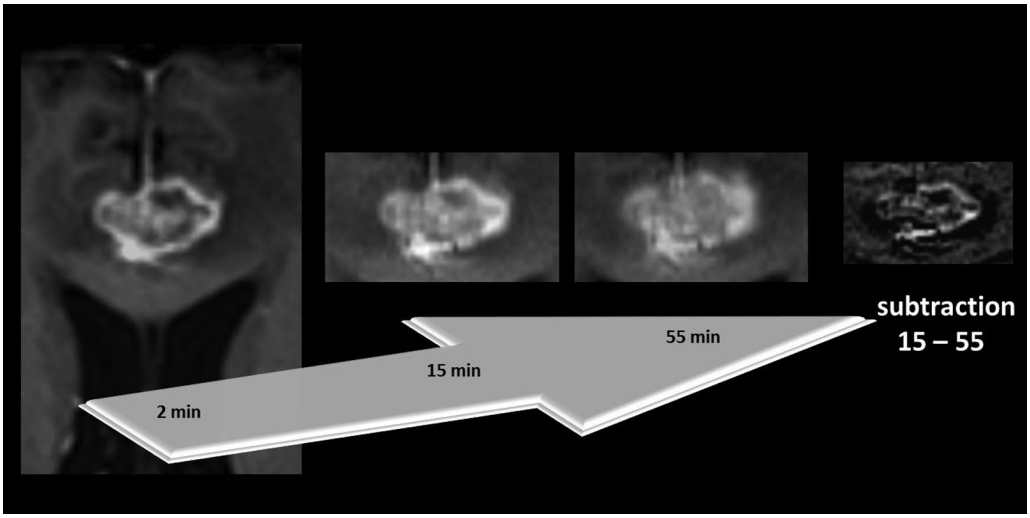

Fig. 2 Tumor recurrence in a 68-year-old man with a metastasis from renal cancer treated with SRS. From left to right, axial T1-weighted MR images 2min, 15min, and 55min after contrast agent administration with subtraction image 15min minus 55min.The subtraction image shows—in contrast to the radiation-induced injury in Fig. 1—white components in the inner area of the lesion. The border of the lesion is still sharp 15min after injecting contrast. Although the lesion loses signal intensity from 15min to 55min, the signal intensity contrast between the rim and the inner area remains for up to 55min.

presence of a signal of the rim or regarding a signal of the entire rim (Fig. 3A).

Evaluation of the subtraction images was in line with the results of the visual analysis of SI changes: all lesions of the radiation-induced injury group showed a further increase in SI of the interior area from 15min to 55min, whereas SI decreased in all malignant lesions ($P < .001$). This change was preceded by an increase in SI in all lesions without an intergroup difference from 2min to 15min (Fig. 3B).

Two radiation-induced injuries and 5 newly diagnosed distant metastases showed a solid, homogeneous contrast enhancement at 2min. Thirty-five of the 41 lesions showed a rim enhancement with an interior area of low signal. The total area increased in all lesions from 2min to 55min; a more pronounced increase was found in the malignancy group with a significant difference for the diagnostic groups for the quotient of the total area 55min to 15min and 55min to 2min ($P < .001$) (Fig. 4). In contrast, the size of the inner area decreased from 2min to 55min and the rim area increased in the radiation-induced injury group ($P < .001$) (Figs. 4, 5). Additionally, lesions in the radiation-induced injury group showed decreasing SI contrast between the rim and the interior area from 2min to 15min and from 15min to 55min, whereas the difference in SI contrast remained clearly visible in the malignancy group ($P < .001$) (Fig. 5).

A further significant interaction effect between time point and diagnosis was found for the margin of the lesion: a progressive blurring of lesion margins was found in the radiation-induced injuries group already at 2min up to 15min, while malignant lesions still showed a sharp margin at 15min ($P < .001$).

Leptomeningeal enhancement was only seen in malignancies (4), and solid parts of the rim were seen in 9.8% of radiation-induced injuries and 38.7% of malignancies, which did not reach level of significance for either diagnostic group (Fig. 3C). Additionally, no significant difference was found for the diagnostic groups regarding the presence of feeding vessels and the structure of the interior area.

Discussion

In this study we have shown that the time-dependent changes in lesion morphology are characteristic and significantly different for malignancies and radiation-induced injuries after SRS to treat brain metastases. All malignant lesions lose SI from 15min to 55min, while the margin is sharply delineated up to 15min after contrast agent administration, and the SI contrast at the rim and interior area can still be detected for up to 55min. Radiation-induced injuries, on the other hand, show a decreasing SI contrast between the rim and the interior area, with a progressive, centripetal contrast enhancement and an increase in SI of the interior area from 15min to 55min. We recommend performing subtraction images 15min minus 55min, which provide information about the SI time course at a glance: radiation-induced injuries show a homogeneous, dark interior area of the lesion, whereas malignant lesions show white components.

There is a large overlap between the radiation-induced injuries and malignancy when the morphology of the lesions is analyzed at a single and an early time point after

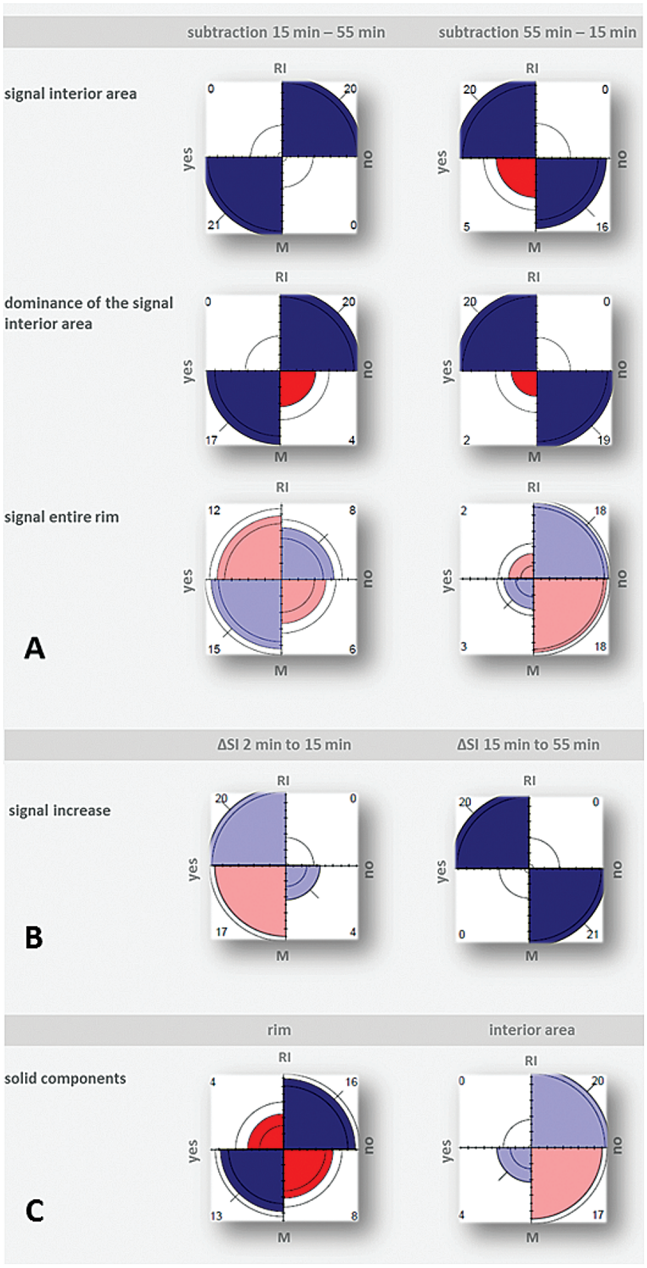

Fig. 3 Fourfold display for qualitative analysis of images per diagnosis (RI = radiation-induced injury; M = malignancy). Association between the 2 respective variables (measured by the sample odds ratio of their 2-by-2 table) is depicted by the tendency of diagonally opposite quarter circles in one direction to differ in area from those in the other direction. The direction of positive association is indicated by blue color and thick diagonal marks, where darker colors highlight displays with a significant association. In addition, the absolute frequencies in the underlying 2-by-2 table are printed in the corners of each display.A: Diagnosis and qualitative parameters (first to third row) of subtraction images 15min minus 55min (left column) and of subtraction image 55min minus 15min (right column). B: Diagnosis and increase in signal intensity from 2min to 15min (left) and 15min to 55min (right), respectively. C: Diagnosis and location of solid components.Signal interior area and dominance of the signal in the interior area of each direction of subtraction (A) and signal increase from 15min to 55min after contrast administration (B) depend significantly on the diagnosis (Holm-adjusted *P*-value < 0.001).

contrast agent administration, as is the case in most routine examinations. Necrotic foci, contrast enhancement, and perilesional edema are the most frequently reported MRI features for radiation-induced necrosis[14–19]—features that are commonly present in recurrent tumor as well. In the study by Dequesada et al,[10] all conventional radiographic features, namely arteriovenous shunting, gyriform distribution, patterns of enhancement resembling

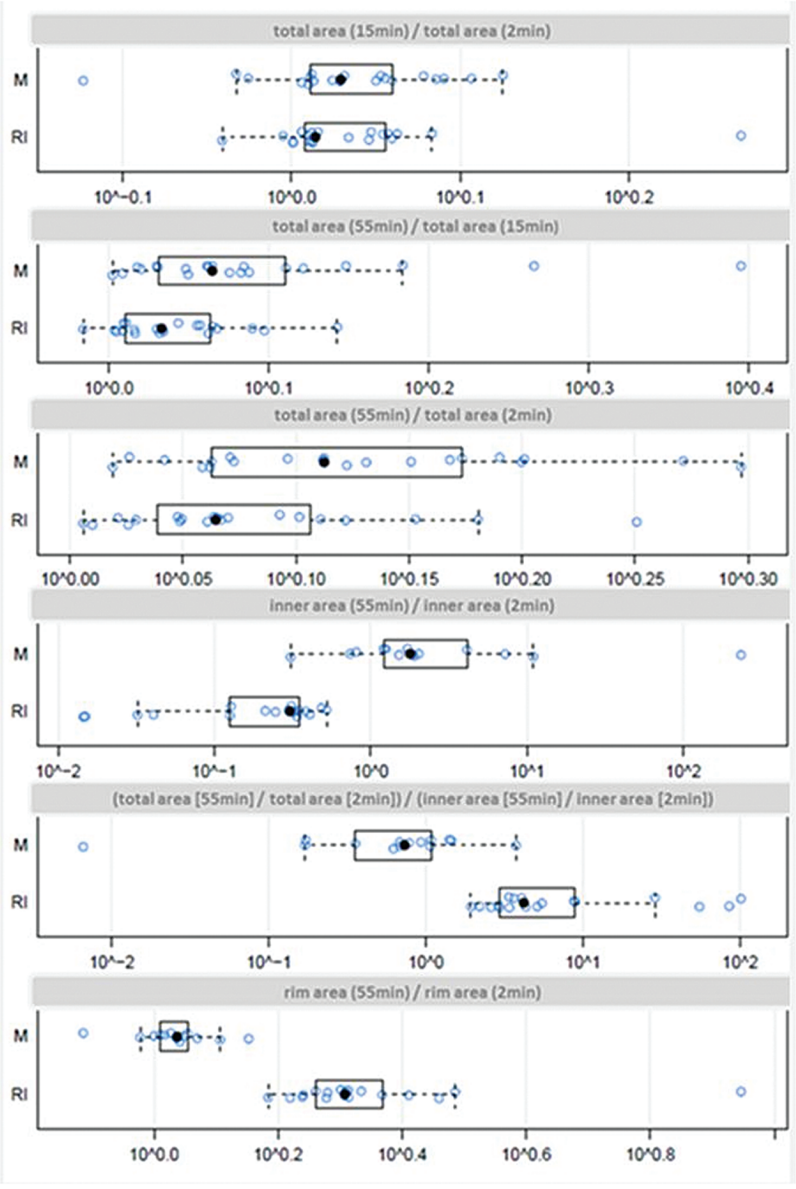

Fig. 4 Quantitative area measurements. Univariate scatterplots including superimposed boxplots of the quotient of the area measurements from 2 different time points after administration of contrast agent per diagnosis (M = malignancy; RI = radiation-induced injury). The edges of the box represent the 25th and 75th percentiles. The scattered line on each box indicates the range of data distribution. Further circles represent outliers (values 1.5 box length from the 75th and 25th percentiles). Decadic logarithmic scale of values.The total area increased in all lesions from 2min to 55min with a significant difference for the diagnostic groups for the quotient of the total area 55min to 15min and 55min to 2min (upper three rows). In contrast to malignancies, the size of the inner area decreases from 2min to 55min after contrast agent application, while the rim area increases in the radiation-induced injury group ($P < .001$) (lower 3 rows).

"Swiss cheese" or "cut green pepper," edema, and cyst formation had low specificity. Being aware of the limitations of the aforementioned features, additional visual and quantitative analyses were performed on standard MRI studies comparing T2-weighted and contrast-enhanced T1-weighted images. Kano et al[9] found that a visual "T1/T2 mismatch"—lack of a clear and defined lesion margin on T2-weighted compared with the sharply delineated margins on T1-weighted images—predicts a radiation-induced injury with a sensitivity of 83% and a specificity of 91%. Indeed, a lesion quotient of 0.6 or greater was seen in all cases of recurrent tumor; a lesion quotient greater than 0.3 was seen in 19 of 20 cases of combined recurrent tumor and radiation-induced injury; and a lesion quotient of 0.3 or less was seen in 4 of 5 cases of radiation necrosis. In the study by Dequesada et al, the "lesion quotient"

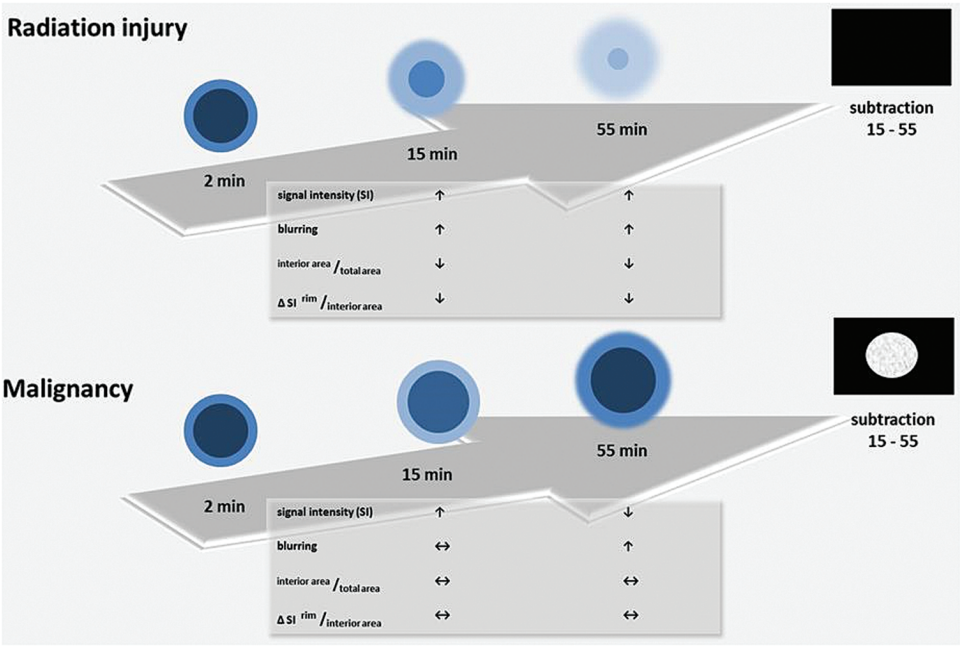

Fig. 5 Schematic diagram of time-dependent changes in lesion morphology on sequential MRI for up to 55 minutes in radiation-induced injury (upper row) and malignancy (lower row). Characteristic time-dependent changes in lesion morphology per diagnosis are summarized in the tables and shown schematically in the graphics on T1-weighted images 2min, 15min, and 55min after intravenous contrast administration and on the subtraction images 15min minus 55min.On the subtraction images radiation-induced injuries show a homogeneous, black interior area of the lesion, whereas all malignant lesions show white components.

(LQ)—proportional value maximum cross-sectional area on T2-weighted to T1-weighted after contrast enhancement with gadolinium—appears to reliably identify radiation necrosis on standard-sequence MRI (sensitivity of 80% and specificity of 96%).[10] However, this is still a controversial debate. Stockham et al could not confirm these findings.[11] Their data, which included a larger number of patients, revealed that specificity for LQ was acceptable (91%) but the sensitivity poor (8%) for determining radiation-induced necrosis. The test was neither sensitive (0%) nor specific (64%) for the combination of recurrent tumor and radiation necrosis, and inadequately sensitive (59%) and specific (41%) for determining recurrent tumor only.

Contrary to these previous studies, we analyzed the time-dependent changes in the morphology of lesions for up to 55min after administering contrast agent. Ludemann et al proposed a model of processes responsible for contrast medium exchange between blood and tissue: the slowly enhancing compartment in tumors probably relates to necrotic processes, whereas the rapidly enhancing compartment indicates supply of viable tissue.[22,31] We surmise that the delayed enhancement in radiation-induced injuries in our patients corresponds to the slow enhancement pattern presented in this model. Our results are also in line with the study by Zach et al.[32] These authors distinguished between tumoral and nontumoral tissues in various types of brain tumors by calculating treatment response assessment maps with fast and slow clearance rates of the contrast agent between an early time point (2min) and a delayed time point (75min). They found that, histologically, the common feature in vessel morphology in the rapidly enhancing regions was the undamaged vessel lumen as tumor tissue, while vessels in the slowly enhancing regions represented significantly damaged lumina secondary to radiation-induced endothelial damage. These findings may help to explain the different SI time courses of radiation-induced injuries and tumor recurrence/tumor progression in our study. They may further explain the phenomenon of the progressive contrast "fill in" up to 55min in radiation-induced injuries, as well as the persistent sharpness of the rim in malignancy for up to 15min. In contrast to the work by Zach et al, our study group is more homogeneous, comprising only patients with SRS-treated metastases. Instead of using institutionally developed maps, our subtraction images 15min minus 55min provide the information about the SI time course at a glance. If a patient leaves the scanner between the 2 measuring time points, autoalignment must be assured. Additionally in our concept, we analyzed the time-dependent changes in lesion morphology and found them to be characteristic and statistically significantly different.

There are limitations to this study. The number of lesions that ultimately were included is small. In the final statistical analysis 41 lesions could be included. Another limitation is that we did not obtain histological proof in our patients. The long observation period over 4 years in our study, however, should justify the assignment to a diagnostic group based on repeated follow-up MRI. By applying our

concept, the late images (at 55min) are essential to make the correct diagnosis. For practical reasons in a clinical setting we suggest returning the patient to the scanner for the short delayed scan. Finally, we did not compare our results of sequential, contrast-enhanced MRI with other modalities, such as PET-CT, which might better support the usefulness of our method.

Conclusions

Analysis of time-dependent changes in lesion morphology on sequential MRI up to 55min after contrast administration appears to be a reliable tool to distinguish radiation-induced injuries from tumor progression. This approach is easily reproducible and might be helpful in planning therapy in the follow-up of patients after SRS for brain metastases.

We recommend performing subtraction images 15min minus 55 min: radiation-induced injuries show a homogeneous, black inner area of the lesion, whereas all malignant lesions show white components.

Funding

None.

Conflict of interest statement. All authors stated no financial relationship to disclose. All authors stated no conflicts of interest to declare.

References

1. Karlsson B, Hanssens P, Wolff R, et al. Thirty years' experience with stereotactic surgery for metastases to the brain. *J Neurosurg*. 2009;111(3):449–457.
2. Wen PY, Macdonald DR, Reardon DA, et al. Updated response assessment criteria for high-grade gliomas: response assessment in Neuro-Oncology working group. *J Clin Oncol*. 2010;28(11):1963–1972.
3. Miot E, Hoffschir D, Alapetite C, et al. Experimental MR study of cerebral radiation injury: quantitative T2 changes over time and histopathologic correlation. *AJNR Am J Neuroradiol*. 1995;16(1):79–85.
4. Kang TW, Kim ST, Byun HS, et al. Morphological and functional MRI, MRS, perfusion and diffusion changes after radiosurgery of brain metastasis. *Eur J Radiol*. 2009;72(3):370–80.
5. Bobek-Billewicz B, Stasik-Pres G, Majchrzak H, et al. Differentiation between brain tumor recurrence and radiation injury using perfusion, diffusion-weighted imaging and MR spectroscopy. *Folia Neuropathol*. 2010;48(2):81–92.
6. Mitsuya K, Nakasu Y, Horiguchi S, et al. Perfusion weighted magnetic resonance imaging to distinguish the recurrence of metastatic brain tumors from radiation necrosis after stereotactic radiosurgery. *J Neurooncol*. 2010;99(1):81–88.
7. Barajas RF, Chang JS, Sneed PK, et al. Distinguishing recurrent intra-axial metastatic tumor from radiation necrosis following gamma knife radiosurgery using dynamic susceptibility-weighted contrast-enhanced perfusion MR imaging. *AJNR Am J Neuroradiol*. 2009;30(2):367–372.
8. Lizarraga KJ, Allen-Auerbach M, Czernin J, et al. (18)F-FDOPA PET for differentiating recurrent or progressive brain metastatic tumors from late or delayed radiation injury after radiation treatment. *J Nucl Med*. 2014;55(1):30–36.
9. Kano H, Kondziolka D, Lobato-Polo J, et al. T1/T2 matching to differentiate tumor growth from radiation effects after stereotactic radiosurgery. *Neurosurgery*. 2010;66(3):486–91.
10. Dequesada IM, Quisling RG, Yachnis A, et al. Can standard magnetic resonance imaging reliably distinguish recurrent tumor from radiation necrosis after radiosurgery for brain metastases? A radiographic-pathological study. *Neurosurgery*. 2008;63(5):898–903.
11. Stockham AL, Tievsky AL, Koyfman SA, et al. Conventional MR imaging does not reliably distinguish radiation necrosis from tumor recurrence after stereotactic radiosurgery. *J Neurooncol*. 2012;109(1):149–158.
12. Heye AK, Culling RD, Valdés Hernández Mdel C, et al. Assessment of blood-brain barrier disruption using dynamic contrast-enhanced MRI. A systematic review. *Neuroimage Clin*. 2014;6:262–74.
13. Mahrholdt H, Wagner A, Judd RM, et al. Delayed enhancement cardiovascular magnetic resonance assessment of non-ischaemic cardiomyopathies. *Eur Heart J*. 2005; 26(15):1461–1474.
14. Chan YL, Leung SF, King AD, et al. Late radiation injury to the temporal lobes: morphologic evaluation at MR imaging. *Radiology*. 1999;213(3):800–807.
15. Valk PE, Dillon WP. Radiation injury of the brain. *AJNR Am J Neuroradiol*. 1991;112(1):45–62.
16. Curran WJ, Hecht-Leavitt C, Schut L, et al. Magnetic resonance imaging of cranial radiation lesions. *Int J Radiat Oncol Biol Phys*. 1987;13(7):1093–1098.
17. Dooms GC, Hecht S, Brant-Zawadzki M, et al. Brain radiation lesions: MR imaging. *Radiology*. 1986;158(1):149–155.
18. Valk PE, Dillon WP. Diagnostic imaging of central nervous system radiation injury. In: Gutin PH, Leibel SA, Sheline GE, eds. *Radiation Injury to the Nervous System*. New York: Raven Press Ltd.; 1991:211–237.
19. Van Tassel P, Bruner JM, Maor MH, et al. MR of toxic effects of accelerated fractionation radiation therapy and carboplatin chemotherapy for malignant gliomas. *AJNR Am J Neuroradiol*. 1995;16(4):715–726.
20. Mathews VP, Caldemeyer KS, Ulmer JL, et al. Effects of contrast dose, delayed imaging, and magnetization transfer saturation on gadolinium-enhanced MR imaging of brain lesions. *J Magn Reson Imaging*. 1997;7(1):14–22.
21. Israeli D, Tanne D, Daniels D, et al. The application of MRI for depiction of subtle BBB disruption in stroke. *Int J Biol Sci*. 2010;7(1):1–8.
22. Lüdemann L, Grieger W, Wurm R, et al. Quantitative measurement of leakage volume and permeability in gliomas, meningiomas and brain metastases with dynamic contrast-enhanced MRI. *Magn Reson Imaging*. 2005;23(8):833–41.
23. Schorner W, Laniado M, Niendorf HP, et al. Time-dependent changes in image contrast in brain tumors after gadolinium-DTPA. *AJNR Am J Neuroradiol*. 1986;7(6):1013–1020.
24. R Core Team. (2013) R: A language and environment for statistical computing. Available at http://www.R-project.org/. Accessed 2013.
25. Bates D, Maechler M, Bolker B, et al. (2014) lme4: Linear mixed-effects models using Eigen and S4. Available at http://CRAN.R-project.org/package=lme4. Accessed 2014.

26. Pinheiro JC, Bates DM, eds. *Mixed-Effects Models in S and S-PLUS*. Corr. 2nd ed. New York: Springer; 2001.

27. Brown H, Prescott R. *Applied Mixed Models in Medicine*. Chichester: John Wiley & Sons Ltd; 1999.

28. Diggle PJ, Heagerty PJ, Liang KY, et al, eds. *Analysis of Longitudinal Data*. 2nd ed. Oxford: Oxford Universiy Press; 2002.

29. Brunner E, Langer F. Nonparametric analysis of ordered categorical data in designs with longitudinal observations and small sample sizes. *Biom J*. 2000; 42(6):663–675.

30. Friendly M. (1995) A fourfold display for 2 by 2 by k tables. Available at http://datavis.ca/papers/4fold/4fold.pdf. Accessed 1995.

31. Tofts PS, Kermode AG. Measurement of the blood-brain barrier permeability and leakage space using dynamic MR imaging. 1. Fundamental concepts. *Magn Reson Med*. 1991;17(2):357–367.

32. Zach L, Guez D, Last D, et al. Delayed contrast extravasation MRI: a new paradigm in neuro-oncology. *Neuro Oncol*. 2015;17(3):457–65.